INTERNATIONAL JOURNAL OF CIRCUIT THEORY AND APPLICATIONS
Int. J. Circ. Theor. Appl. 2017; **45**:1833–1848
Published online 27 July 2017 in Wiley Online Library (wileyonlinelibrary.com). DOI: 10.1002/cta.2353

Control and synchronization of the generalized Lorenz system with mismatched uncertainties using backstepping technique and time-delay estimation

Dongwon Kim[1], Maolin Jin[2] and Pyung Hun Chang[3,*,†]

[1]*Department of Mechanical Engineering, University of Michigan, Ann Arbor, MI, USA*
[2]*Korea Institute of Robot and Convergence (KIRO), Pohang, Gyeongbuk, Korea*
[3]*Department of Robotics Engineering, Daegu-Gyeongbuk Institute of Science and Technology (DGIST), Daegu, Korea*

SUMMARY

We propose a robust control technique for regulation and synchronization of the generalized Lorenz system (GLS) that covers the Lorenz system, Chen system and Lü system. The proposed control provides synergy through the combination of the backstepping control and *time-delay estimation* (TDE) technique. TDE is used to estimate and cancel nonlinearities and uncertainties while the backstepping method is adopted to provide robustness against matched and mismatched uncertainties. As a result, we observe in numerical simulation that the proposed technique shows better performances in regulating and synchronizing the GLS with mismatched uncertainties, in comparison with existing schemes. The efficacy of the proposed technique is also validated with a circuit-implemented chaotic system. Copyright © 2017 John Wiley & Sons, Ltd.

Received 7 March 2017; Revised 16 March 2017; Accepted 20 March 2017

KEY WORDS: chaotic system; robust control; synchronization; chaotic circuit; time-delay estimation; backstepping

1. INTRODUCTION

Chaotic behaviors provide various applications based on their irregularity and unpredictability. These applications are shown in various fields, including physical, chemical and ecological systems, and secure communications [1–3]. Correspondingly, a variety of control theories have been applied to managing chaotic signals [4–20]. Recently, for a faster response and enhanced robustness, hybrid methods have appeared in regulating and synchronizing chaotic systems. For example, adaptive control and backstepping technique are combined in [9,21, 22], optimal control and sliding mode control are used together in [12], and fuzzy logic, adaptive control and sliding mode control are merged in [10,13,17,23]. These approaches, however, require a precise chaotic system model and are vulnerable to parameter variations, modeling errors and external disturbances. Moreover, these hybrid methods are quite complicated.

In 2008, Jin and Chang incorporated the time-delay estimation (TDE) technique to obtain simplicity and robustness [24]. Jin and Chang's strategy comprises three parts: a TDE part to cancel the controlled system's dynamics, an injection part to endow the desired master system's dynamics and a convergence part to shape the synchronization error dynamics. It provides fast, accurate and robust

*Correspondence to: Pyung Hun Chang, Department of Robotics Engineering, Daegu-Gyeongbuk Institute of Science and Technology (DGIST), Daegu 711-873, Korea.
†E-mail: phchang@dgist.ac.kr

performance. With the TDE technique, Kim et al. also proposed a regulation and synchronization method using terminal sliding mode (TSM) [25]. Kim's method achieves fast and powerful convergence. The aforementioned two methods based on the TDE technique do not include a suppression of mismatched uncertainties, however, which make them vulnerable when matching conditions are not satisfied.

Suppressing the effect of mismatched uncertainties is important in minimizing the number of control inputs and sensors. In this paper, we propose a simple robust technique that is able to care of mismatched uncertainties in a chaotic system as well as matched uncertainties through the combination of the backstepping technique and TDE technique. The backstepping method enables a systematic and recursive procedure for the design of control laws for systems in strict feedback form, while the TDE technique enables a simple effective compensation for uncertainties. Therefore, the proposed technique provides a single controller that can be applied to any systems in strict feedback form even if a precise system model is not identified. In addition to this benefit, uncertainties that reside on each equation of a chatic system can be suppressed by one TDE and all TDEs of the chaotic system are governed by the control input. The proposed technique is thus expected to be superior in dealing with mismatched uncertainties.

To verify the efficacy of the proposed technique, we apply the technique to the regulation and synchronization problems of the generalized Lorenz system (GLS) introduced in [26, 27]. The GLS covers the well-known classical Lorenz system [28], Chen system [29] and Lü system [30] in one formulation. We perform a comparative study with the TDE-based controllers proposed in the previous works [24, 25].

This study is an extension of our previous work originally reported in our short proceeding [43]. In this paper, we additionally provide the stability analysis for the closed-loop system with the proposed technique and present an experimental study. Experimental implementation is crucial for practical applications of chaos [12,31–34], because the signal is always contaminated by noise. Numerical differentiation of state variables is required to conduct the proposed technique, and it can easily amplify the noise effect; the proposed technique should be verified through an experiment or, at least, computer simulation considering noise. In this paper, we verify the proposed control through physical chaotic systems with analog circuit elements.

This paper begins with the design procedures of controllers, each of which is tailored to the regulation and synchronization problems, respectively, with a brief explanation of the GLS. In the following sections, the proposed controllers are validated through a simulation study and experimental study. We allocate subsections separately to the regulation and synchronization parts as well in these validation studies. Finally, we make remarks in the conclusion section.

2. CONTROLLER DEVELOPMENT

2.1. Regulation

The GLS [2] is described as

$$\dot{\mathbf{x}} = \begin{bmatrix} \mathbf{A} & 0 \\ 0 & \lambda_3 \end{bmatrix} \mathbf{x} + x_1 \begin{bmatrix} 0 & 0 & 0 \\ 0 & 0 & -1 \\ 0 & 1 & 0 \end{bmatrix} \mathbf{x}, \quad \mathbf{A} = \begin{bmatrix} a_{11} & a_{12} \\ a_{21} & a_{22} \end{bmatrix}, \tag{1}$$

where $\mathbf{x} = [x_1 \ x_2 \ x_3]^T$, $\lambda_3 \in \mathbb{R}$ and matrix $\mathbf{A}$ has eigenvalues $\lambda_1, \lambda_2 \in \mathbb{R}, \lambda_{2,3} < 0, \lambda_1 > 0$.

The control objective is to regulate $\mathbf{x}$ to a specific constant $\mathbf{x}_d = \left[x_{1d} \, x_{1d} - \frac{x_{1d}^2}{\lambda_3} \right]^T$. If $x_1(t)$ converges to a specific point x_{1d}, state $x_2(t)$ converges to the specific point x_{1d} as well from the fact that $\dot{x}_1(t) = 0$. Once $x_1(t)$ and $x_2(t)$ converge to point x_{1d}, state $x_3(t)$ converges to a certain point based on the characteristic that

DOI: 10.1002/cta

parameter (eigenvalue) $\lambda_3 < 0$ (Eq. (1)). Considering this fact, we can separate the GLS into two parts as follows:

$$\begin{aligned} &\text{First part}: \begin{cases} \dot{x}_1 = a_{11}x_1 + a_{12}x_2 + d_1, \\ \dot{x}_2 = a_{21}x_1 + a_{22}x_2 - x_1x_3 + d_2, \end{cases} \\ &\text{Second part}: \ \dot{x}_3 = \lambda_3 x_3 + x_1x_2, \end{aligned} \tag{2}$$

where d_1 and d_2 denote unknown disturbances, which are assumed to be continuous and bounded.

Now, it is required to control the first part of the GLS to achieve the control objective. The control of the first part can be achieved by adding a control input u to the differential equation of state x_2. In order to design a robust backstepping technique, we transform the first part of Eqs. (2) as follows:

$$\begin{cases} \dot{x}_1 = a_{11}x_1 + a_{12}x_2 + d_1, \\ \dot{x}_2 = a_{21}x_1 + a_{22}x_2 - x_1x_3 + d_2 + u,. \end{cases} \Rightarrow \begin{cases} \dot{x}_1 = f_1 + g_1x_2, \\ \dot{x}_2 = f_2 + g_2u, \end{cases} \Rightarrow \begin{cases} \dot{x}_1 = h_1 + \hat{g}_1x_2, \\ \dot{x}_2 = h_2 + \hat{g}_2u, \end{cases} \tag{3}$$

where

$$\begin{aligned} &f_1 = a_{11}x_1 + d_1, g_1 = a_{12}, \\ &f_2 = a_{21}x_1 + a_{22}x_2 - x_1x_3 + d_2, g_2 = 1, \end{aligned} \tag{4}$$

and h_i $(i = 1, 2)$ are terms that include all uncertainties:

$$\begin{aligned} h_1 &= a_{11}x_1 + (a_{12} - \hat{g}_1)x_2 + d_1, \\ h_2 &= a_{21}x_1 + a_{22}x_2 - x_1x_3 + d_2 + (1 - \hat{g}_2)u, \end{aligned} \tag{5}$$

where $\hat{g}_1$ and $\hat{g}_2$ are constants.

With a definition $e_1 \triangleq x_{1d} - x_1$, a Lyapunov function V_1 can be designed as

$$V_1 \triangleq \frac{1}{2}{e_1}^2. \tag{6}$$

The time derivative of V_1 is

$$\dot{V}_1 = e_1\dot{e}_1 = e_1(\dot{x}_{1d} - h_1 - \hat{g}_1x_2). \tag{7}$$

From Eq. (7), treating x_2 as a virtual control effort, the 'desired control effort value x_{2d}' for x_2 is chosen so that the negative definiteness of $\dot{V}_1$ is guaranteed.

$$\begin{aligned} &\dot{V}_1 = -C_1e_1^2, \\ &x_{2d} \triangleq \hat{g}_1^{-1}(\dot{x}_{1d} + h_1 + C_1e_1), \end{aligned} \tag{8}$$

where C_1 is a design parameter.

Because $x_{2d} = \hat{g}_1^{-1}(\dot{x}_{1d} - h_1 + C_1e_1)$ is a desired control effort and differs from the real state x_2, we denote this 'desired control effort value'. The next step of the proposed design is to make the error between x_2 and x_{2d} as small as possible. The actual control effort is designed so that the error between x_2 and x_{2d} converges to zero. The error between x_2 and x_{2d} is defined as follows:

DOI: 10.1002/cta

$$e_2 \triangleq \hat{g}_1(x_{2d} - x_2). \tag{9}$$

We define a Lyapunov function candidate V_2 as

$$V_2 \triangleq \frac{1}{2} e_2^2. \tag{10}$$

Differentiating V_2 with respect to time gives

$$\dot{V}_2 = e_2\dot{e}_2 = e_2\hat{g}_1(\dot{x}_{2d} - \dot{x}_2) = e_2\left(\ddot{x}_{1d} - \dot{h}_1 + C_1\dot{e}_1 - \hat{g}_1 h_2 - \hat{g}_1\hat{g}_2 u\right) = -C_2 e_2^2. \tag{11}$$

From Eq. (7), the actual control effort is chosen so that the negative definiteness of $\dot{V}_2$ is guaranteed, as follows:

$$u = (\hat{g}_1\hat{g}_2)^{-1}\left(\ddot{x}_{1d} + \hat{g}_1 h_2 + \dot{h}_1 + C_1\dot{e}_1 + C_2 e_2\right), \tag{12}$$

where C_2 is a design parameter.

Now, we need to estimate the value of the term $\hat{g}_1 h_2 + \dot{h}_1$. Differentiating the first equation of Eqs. (3) with respect to time gives

$$\ddot{x}_1 = \dot{h}_1 + \hat{g}_1 h_2 + \hat{g}_1\hat{g}_2 u = H + \overline{B}u, \tag{13}$$

where $H \triangleq \hat{g}_1 h_2 + \dot{h}_1, \overline{B} \triangleq \hat{g}_1\hat{g}_2$.

With the assumption that d_1 and d_2 are continuous, it is reasonable to regard H as a continuous function. It is obvious that the states of the GLS are continuous (see Eq. (1)). Then, we could build an approximation $H(t) \cong H(t-L)$, provided that the sampling period L is sufficiently small. This estimation, called TDE [35–42], is formally defined as

$$\hat{H}(t) = H(t-L). \tag{14}$$

For a practical use, the estimate of the term H can be obtained as, using Eq. (13),

$$\hat{H}(t) = H(t-L) = \ddot{x}_1(t-L) - \overline{B}^{-1}u(t-L). \tag{15}$$

The estimate is obtained by using the previous-step sensor reading and record of the previous-step input. If time delay L is sufficiently small, the nonlinearities and uncertainties of the system dynamics can be estimated and canceled out using TDE. [35–42]. Therefore, the TDE technique provides simplicity and robustness against uncertainties without substantial computation loads. Substituting Eq. (15) into Eq. (12) with the relationship $e_2 = \dot{e}_1 + C_1 e_1$ leads to the final form of the actual control input as follows:

$$u = u(t-L) + \overline{B}^{-1}(\ddot{x}_{1d} - \ddot{x}_1(t-L) + (C_1 + C_2)\dot{e}_1 + C_1 C_2 e_1). \tag{16}$$

Control gains C_1 and C_2 determine how fast the error e_1 converges. In Eq. (16), the delayed acceleration is calculated by numerical differentiation [35–42], as $\ddot{x}_1(t-L) = (x_1(t) - 2x_1(t-L) + x_1(t))/L^2$.

2.2. *Stability analysis*

The stability analysis of the overall closed-loop system is performed and the sufficient condition for closed-loop stability is derived. If the exact value of H was able to be identified, the closed-loop system with the control input would be asymptotically stable, based on the Lyapunov stability theorem. However, because the value of H is estimated using TDE, stability is not guaranteed due to

DOI: 10.1002/cta

the difference between the real value of H and its estimate. Here, we analyze the stability of the closed-loop system taking the difference into account, grounded on the proof presented in [42].

$$u_{(t)} = \overline{B}^{-1}\left[v_{(t)} - \hat{H}_{(t)}\right], \tag{17}$$

where $v_{(t)} \triangleq \ddot{x}_{1d(t)} + (C_1 + C_2)\dot{e}_{1(t)} + C_1C_2e_{1(t)}$.

Differentiating the first equation of (3) with respect to time gives

$$\ddot{x}_{1(t)} = H_{(t)} + \overline{B}u_{(t)}. \tag{18}$$

Substituting Eq. (17) into Eq. (18) yields

$$\ddot{x}_{1(t)} - v_{(t)} = H_{(t)} - \hat{H}_{(t)}. \tag{19}$$

With TDE error $\varepsilon_{(t)}$ defined as

$$\varepsilon_{(t)} \triangleq v_{(t)} - \ddot{x}_{1(t)} = \hat{H}_{(t)} - H_{(t)}, \tag{20}$$

we obtain the error dynamics of the proposed control:

$$\ddot{e}_{1(t)} + (C_1 + C_2)\dot{e}_{1(t)} + C_1C_2e_{1(t)} = \varepsilon_{(t)}. \tag{21}$$

From the error dynamics, tracking error $e_{1(t)}$ is influenced by TDE error $\varepsilon_{(t)}$. If $\varepsilon_{(t)}$ is asymptotically bounded, then the error dynamics is also asymptotically bounded [42], and consequently the overall closed-loop system is stable. Therefore, we focus on the boundedness of $\varepsilon_{(t)}$ from now on. To this end, a differential equation representing the dynamics of $\varepsilon_{(t)}$ is derived.

$\ddot{x}_{1(t)}$in Eq. (3) can be arranged as follows:

$$\ddot{x}_{1(t)} = a_{(t)} + B_{(t)}u_{(t)}, \tag{22}$$

where

$$a_{(t)} = \dot{f}_{1(t)} + \dot{g}_{1(t)}x_{2(t)} + g_{1(t)}f_{2(t)}, \tag{23}$$

$$B_{(t)} \triangleq g_{1(t)}g_{2(t)}. \tag{24}$$

The combination of Eq. (18) with Eq. (22) gives

$$H_{(t)} = a_{(t)} + \left[B_{(t)} - \overline{B}\right]u_{(t)}. \tag{25}$$

Using Eq. (20), we can arrange Eq. (25) as follows:

$$\varepsilon_{(t)} = H_{(t-L)} - H_{(t)} = a_{(t-L)} + \left[B_{(t-L)} - \overline{B}\right]u_{(t-L)} - \left(a_{(t)} + \left[B_{(t)} - \overline{B}\right]u_{(t)}\right). \tag{26}$$

Substituting Eqs. (15) and (19) into Eq. (26) gives

$$\varepsilon_{(t)} = a_{(t-L)} - a_{(t)} + \left[B_{(t-L)} - \overline{B}\right]u_{(t-L)} - \left[B_{(t)} - \overline{B}\right]\left[u_{(t-L)} + \overline{B}^{-1}\left(-\ddot{x}_{1(t-L)} + v_{(t)}\right)\right]. \tag{27}$$

From the above equations, we derive the following relationships:

DOI: 10.1002/cta

$$u_{(t-L)} = \overline{B}^{-1}\left[\ddot{x}_{(t-L)} - a_{(t)}\right], \tag{28}$$

and

$$\ddot{x}_{1(t-L)} = a_{(t-L)} - \varepsilon_{(t-L)}. \tag{29}$$

Finally, substituting Eqs. (28) and (29) into Eq. (27) and rearranging it give

$$\varepsilon_{(t)} = \left[I - B_{(t)}\overline{B}^{-1}\right]\varepsilon_{(t-L)} + \eta_{1(t-L)} + \left[I - B_{(t)}\overline{B}^{-1}\right]\eta_{2(t-L)}, \tag{30}$$

where

$$\eta_{1(t-L)} = \left[I - B_{(t)}B^{-1}_{(t-L)}\right]\left[x^{(n)}_{(t-L)} - a_{(t)}\right] + a_{(t-L)} - a_{(t)}, \tag{31}$$

$$\eta_{2(t-L)} = v_{(t)} - v_{(t-L)}. \tag{32}$$

Taking the same approach presented in [42], the dynamics of $\boldsymbol{\varepsilon}_{(t)}$ in Eq. (30) can be closely approximated by the dynamics behavior of the following sampled-data system (typically, control is carried out in the digital environment):

$$\varepsilon_{(k)} = \left[I - B_{(k)}\overline{B}^{-1}\right]\varepsilon_{(k-1)} + \eta_{1(k-1)} + \left[I - B_{(k)}\overline{B}^{-1}\right]\eta_{2(k-1)}. \tag{33}$$

Equation (33) is a first-order time-varying difference equation in which $\eta_{1(k-1)}$ and $\eta_{2(k-1)}$, from the viewpoint of $\boldsymbol{\varepsilon}_{(k)}$, are viewed as external inputs acting as disturbances. Next, we establish a sufficient condition for the convergence of $\boldsymbol{\varepsilon}_{(k)}$ based on Eq. (33). We assume that the convergence of $\boldsymbol{\varepsilon}_{(k)}$ implies the convergence of $\varepsilon_{(t)}$ [4]. We further assume that η_1 and η_2 are bounded, and if the eigenvalues of $I - B_{(k)}\overline{B}^{-1}$ in Eq. (33), denoted by $\xi_{(k)}$, satisfy the condition that $-1 < \xi_{(k)} < 1$, then $\boldsymbol{\varepsilon}_{(k)}$ asymptotically converges to 0. For real systems, $\overline{B}(\triangleq \hat{g}_1\hat{g}_2)$ is dependent on the target system's parameters g_1, g_2 that are difficult and time-consuming to estimate exactly. In practice, $\overline{B}^{-1}$ can be tuned without knowledge of the target system. We would recommend starting with a large positive initial value of $\overline{B}^{-1}$ to tune the system performance.

2.3. Synchronization

Synchronization between two chaotic systems is achieved when each state of a slave chaotic system follows its corresponding state of a master chaotic system. Now, we apply the proposed technique to synchronization between two *identical* chaotic systems with the *different* initial values using one control input.

The master GLS and slave GLS are given as, respectively,

$$\begin{aligned} \dot{x}_{m1} &= a_{11}x_{m1} + a_{12}x_{m2}, \\ \dot{x}_{m2} &= a_{21}x_{m1} + a_{22}x_{m2} - x_{m1}x_{m3}, \\ \dot{x}_{m3} &= \lambda_3 x_{m3} + x_{m1}x_{m2}, \end{aligned} \tag{34}$$

$$\begin{aligned} \dot{x}_{s1} &= a_{11}x_{s1} + a_{12}x_{s2}, \\ \dot{x}_{s2} &= a_{21}x_{s1} + a_{22}x_{s2} - x_{s1}x_{s3}, \\ \dot{x}_{s3} &= \lambda_3 x_{s3} + x_{s1}x_{s2}, \end{aligned} \tag{35}$$

where $\mathbf{x}_m = (x_{m1}, x_{m2}, x_{m3})^T \in R^3$ denotes the state variables of the master system and $\mathbf{x}_s = (x_{s1}, x_{s2}, x_{s3})^T \in R^3$ denotes the state variables of the slave system.

DOI: 10.1002/cta

With the state errors between the slave system and master system defined as

$$e_1 \triangleq x_{s1} - x_{m1}, e_2 \triangleq x_{s2} - x_{m2}, e_3 \triangleq x_{s3} - x_{m3}, \tag{36}$$

the error system can be derived as

$$\begin{aligned} \dot{e}_1 &= a_{11}e_1 - a_{12}e_2, \\ \dot{e}_2 &= a_{21}e_1 + a_{22}e_2 - e_1e_3 - e_1x_{m3} - e_3x_{m1}, \\ \dot{e}_3 &= \lambda_3 e_3 + e_1e_2 + e_1x_{m2} + e_2x_{m1}. \end{aligned} \tag{37}$$

When the error states converge to zero, synchronization between the two systems is achieved. Note that parameter λ_3 is below zero. With the fact that the differential equation of state $e_3(t)$ converges to zero when $e_1(t)$ and $e_2(t)$ converge to zero, the synchronization between the two systems can be achieved by adding a control input to the differential equation of state e_2. That is, the control input is added to the differential equation of state x_{s2} of the slave system.

$$\begin{aligned} &\text{First part :} \quad \begin{cases} \dot{e}_1 = a_{11}e_1 - a_{12}e_2, \\ \dot{e}_2 = a_{21}e_1 + a_{22}e_2 - e_1e_3 - e_1x_{m3} - e_3x_{m1} + u, \end{cases} \\ &\text{Second part :} \quad \dot{e}_3 = \lambda_3 e_3 + e_1e_2 + e_1x_{m2} + e_2x_{m1}. \end{aligned} \tag{38}$$

The proposed control can be designed for the first part of Eqs. (38) with the same procedure of regulation in Section 2. The first part can be rewritten as

$$\begin{aligned} \dot{e}_1 &= h_1 + \hat{g}_1 e_2, \\ \dot{e}_2 &= h_2 + \hat{g}_2 u. \end{aligned} \tag{39}$$

The first part is in the same form with Eq. (3). The control input can be derived as follows in the same way proposed in Section 2:

$$u(t) = u(t-L) + \overline{B}^{-1}(-\ddot{e}_1(t-L) - (C_1 + C_2)\dot{e}_1 - C_1C_2e_1). \tag{40}$$

We emphasize that all uncertainty factors in the first part can be dealt with by TDE as long as they are included in h_1 and h_2.

3. NUMERICAL SIMULATION

3.1. Regulation of the Lorenz system

As an example of the GLS to be controlled, the Lorenz system is chosen. The Lorenz system is simple but captures various features of the GLS. To show the robustness of the proposed controller, we take unstructured uncertainties (i.e., disturbances) as well as structured uncertainties (i.e., parameter variations) into account. Bounded continuous disturbances are considered in the differential equations of state x and state y for more practical circumstances [5]. In addition, the variations of parameters σ, r and b are also considered. Then, the Lorenz system is described as

$$\begin{aligned} \dot{x} &= (\sigma + \delta\sigma)(y - x) + d_1, \\ \dot{y} &= (r + \delta r)x - y - xz + d_2 + u, \\ \dot{z} &= xy - (b + \delta b)z, \end{aligned} \tag{41}$$

where d_1 and d_2 denote disturbances; u a control input; $\delta\sigma, \delta r, \delta b$ the corresponding variations of the parameters σ, r, b, respectively.

DOI: 10.1002/cta

The parameters of the Lorenz system are selected as $\sigma = 10, r = 28$ and $b = 8/3$. The initial values of each system are set to be $(x_0, y_0, z_0) = (10, 0, -10)$. A fourth-order Runge–Kutta method is used to solve the systems with step size 0.0001 s. Parameter L is set to 0.001 s meaning sampling frequency = 1 kHz in the digital implementation. Note that the sampling frequency is sufficiently larger than the Nyquist frequency of the Lorenz system. Design parameters C_1 and C_2 are chosen as 15 to force the error dynamics of the controlled system $\ddot{e}_1 + (C_1 + C_2)\dot{e}_1 + C_1C_2e_1 = 0$ to achieve critical damping. Control gain $\overline{B}$ is tuned to 11. The control input is activated at $t = 5$ s, and the regulation point is designed as $(x_d, y_d, z_d) = (5, 5, 9.375)$, $t \geq 5$ s. The mismatched and matched disturbances are given as $d_1 = \cos(5\pi t)$ and $d_2 = \cos(5\pi t)$, respectively. Parameter variations are set to be $\delta\sigma = 0.1, \delta r = 0.2$ and $\delta b = 0.1$.

The simulation results of the proposed controller are shown in Figure 1. Figure 1a and b display the time responses of the states of the Lorenz system in the presence of the matched uncertainties alone and in the presence of the matched and mismatched uncertainties. The Lorenz system is regulated to the desired state fast and accurately even under the matched disturbance, mismatched disturbance and parameter variations. Figure 1c shows that the errors between x_d and x fall down below ±0.0006 in steady state. To meet the discontinuous shifts of the desired regulation points at $t = 5$ s, the control inputs drastically soar as shown in Figure 1d.

Additionally, we compare the proposed controller with the two TDE-based controllers proposed in [24, 25]. The gains are set as $k_1 = 10$, $k_2 = 50$ for Eq. (10) in [24]; $\alpha = 20$, $\beta = 10$, $\gamma = 0.6$ for Eq. (13) in [25]. Both matched and mismatched uncertainties are considered. Figure 2 shows the responses of state x of the Lorenz system and their corresponding control input u, respectively. The proposed controller shows the smallest steady-state error among the three.

The two controllers proposed in [24, 25] use TDE for only the second equation of the controlled system; mismatched uncertainties on the first equation cannot be suppressed. The proposed

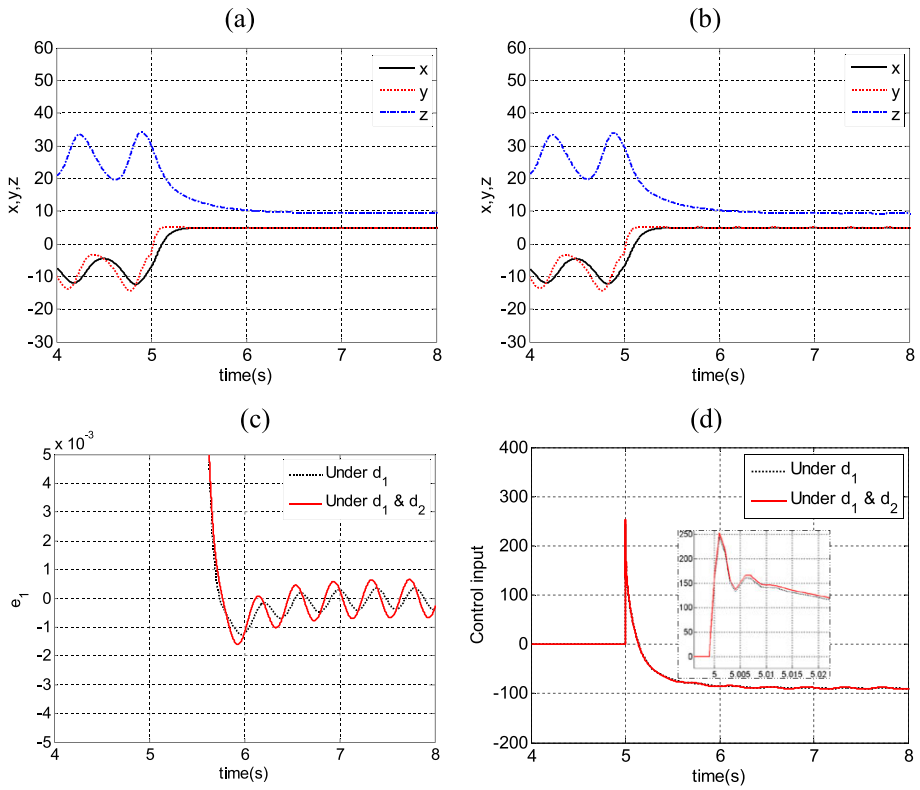

Figure 1. Responses of the Lorenz system in the presence of (a) a matched disturbance and (b) matched, mismatched disturbances. The time evolutions of (c) error states e_1 and (d) control inputs u for the two cases. The control input is exerted at time 5 s. [Colour figure can be viewed at wileyonlinelibrary.com]

DOI: 10.1002/cta

controller can compensate for the mismatched uncertainties by performing TDEs on both the first and second equations.

3.2. *Synchronization of the Lorenz systems*

The Lorenz system is chosen as an example of the GLS as in the regulation case. The master and slave systems can be expressed as, respectively,

$$(x_m, y_m, z_m): \begin{cases} \dot{x}_m = \sigma(y_m - x_m), \\ \dot{y}_m = r x_m - y_m - x_m z_m, \\ \dot{z}_m = x_m y_m - b z_m, \end{cases} \tag{42}$$

and

$$(x_s, y_s, z_s): \begin{cases} \dot{x}_s = \sigma(y_s - x_s), \\ \dot{y}_s = r x_s - y_s - x_s z_s, \\ \dot{z}_s = x_s y_s - b z_s, \end{cases} \tag{43}$$

where $x_m, y_m, z_m \in \Re$ denote the state variables of the master system; $x_s, y_s, z_s \in \Re$ denote the state variables of the slave system; $\sigma, b, r \in \Re$ are parameters.

The initial values of the master system ((x_m, y_m, z_m) in Eq. (42)) are $(x_{m0}, y_{m0}, z_{m0}) = (10, 0, -10)$. The initial values of the slave system ((x_s, y_s, z_s) in Eq. (43)) to be controlled are set as $(x_{s0}, y_{s0}, z_{s0}) = (-10, 0, 10)$. The state variables of the two Lorenz chaotic systems with the different initial values are shown in Figure 3. The parameters of both the Lorenz systems were selected as $\sigma = 10$, $r = 28$, $b = 8/3$. The error system between the master and slave systems can be written as

$$\begin{bmatrix} \dot{e}_x \\ \dot{e}_y \\ \dot{e}_z \end{bmatrix} = \begin{bmatrix} \sigma(e_y - e_x) + \delta\sigma(y_s - x_s) \\ r e_x - e_y - e_x e_z - e_x z_s - e_z x_s + \delta r x_s \\ -b e_z + e_x e_y + e_x y_s + e_y x_s - \delta b z_s \end{bmatrix} + \begin{bmatrix} d_1 \\ d_2 \\ 0 \end{bmatrix} + \begin{bmatrix} 0 \\ 1 \\ 0 \end{bmatrix} u, \tag{44}$$

where $e_x \triangleq x_m - x_s$, $e_y \triangleq y_m - y_s$ and $e_z \triangleq z_m - z_s$.

Bounded disturbances and parameter variations are accommodated as shown in Eq. (44). We assume disturbances as $d_1 = \sin(100z)$ and $d_2 = \cos(100x)$. Parameter variations $\delta\sigma$, δr, and δb are given as 0.1, 0.2 and 0, respectively. The mismatched parameter variation δb is not considered, because it is irrelevant to control performances. Both C_1 and C_2 in Eq. (40) are given as 100 to achieve critical damping when the first error state converses. The larger values of C_1 and C_2 result in the smaller errors. The control input is activated at 3 s, and control gain $\overline{B}$ is tuned to 50.

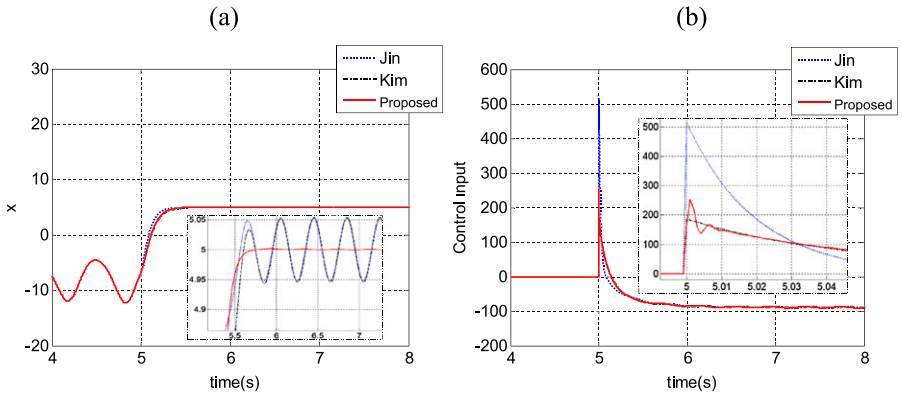

Figure 2. Time evolutions of (a) states *xs* and (b) control inputs *us* with the controllers proposed in [24, 25], and with the proposed control. The control inputs are exerted at time 5 s. [Colour figure can be viewed at wileyonlinelibrary.com]

DOI: 10.1002/cta

The simulation results of synchronization between the two systems are shown in Figure 4. It is observed that the state variables of the slave Lorenz system are synchronized from t = 3 s with the master system, respectively. The trajectories of the states of the master system and slave system tightly overlap each other, respectively. The error states converge to zero fast and accurately even under the matched, mismatched disturbances and parameter variations as shown in Figure 4d. The control input suddenly fluctuates at t = 3 s due to the shifts of the slave system's states toward the desired states at t = 3 s.

We compare the performance of the proposed controller for the synchronization case with that of Kim's controller in [25]. Both of the techniques provide a single controller, which is applied to the second equation of the slave system. The gains are $\alpha = 200$, $\beta = 100$ and $\gamma = 0.6$ for Eq. (31) in [25]. Figure 5 presents the time trajectories of error states and control inputs.

The proposed controller exhibits the better performance in comparison with Kim's controller for error state e_x. This proves the efficacy of the proposed controller in dealing with mismatched uncertainties. Meanwhile, the proposed controller shows the larger synchronization error e_y. This result comes from the fact that the proposed control is originally designed to suppress the first error state, while Kim's controller is designed to suppress only the second error state, assuming that the first and third error equations are internally stable.

4. EXPERIMENT

4.1. Regulation of the Lorenz system

In this section, we validate the proposed technique in controlling a circuit-implemented chaotic system. The Lorenz system is chosen as an example of the GLS. Considering the fact that the state variables of the system occupy a wide dynamic range with values that exceed the reasonable power supply limits of electric elements, we scale variables in a similar way as proposed in [12].With the state scaling factors $x' = x/10, y' = y/10$ and $z' = z/10$, the Lorenz system is scaled down to

$$\begin{aligned} \dot{x}' &= \sigma\left(y' - x'\right), \\ \dot{y}' &= rx' - y' - 10x'z', \\ \dot{z}' &= 10x'y' - bz'. \end{aligned} \tag{45}$$

The state variables have similar dynamic ranges and circuit voltages remain within the range of typical power supply limits. A time-scaling factor should be introduced as $t = G_T\tau$, where G_T denotes a time-scaling factor. Then, the scaled system is expressed as

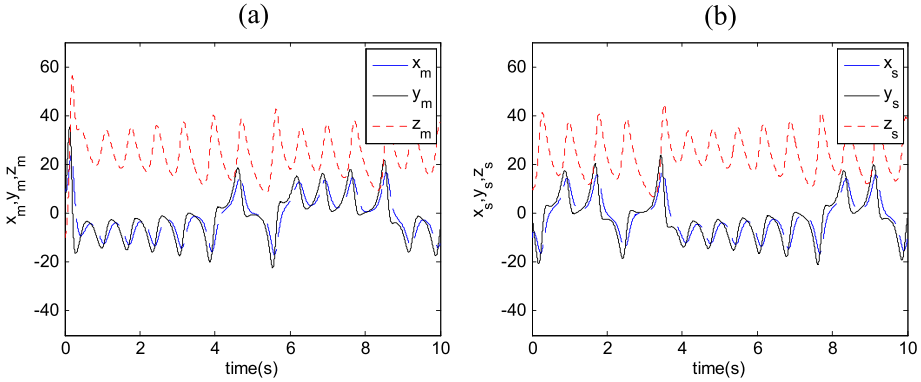

Figure 3. Time evolutions of the states of (a) the master Lorenz system and (b) slave Lorenz system. [Colour figure can be viewed at wileyonlinelibrary.com]

DOI: 10.1002/cta

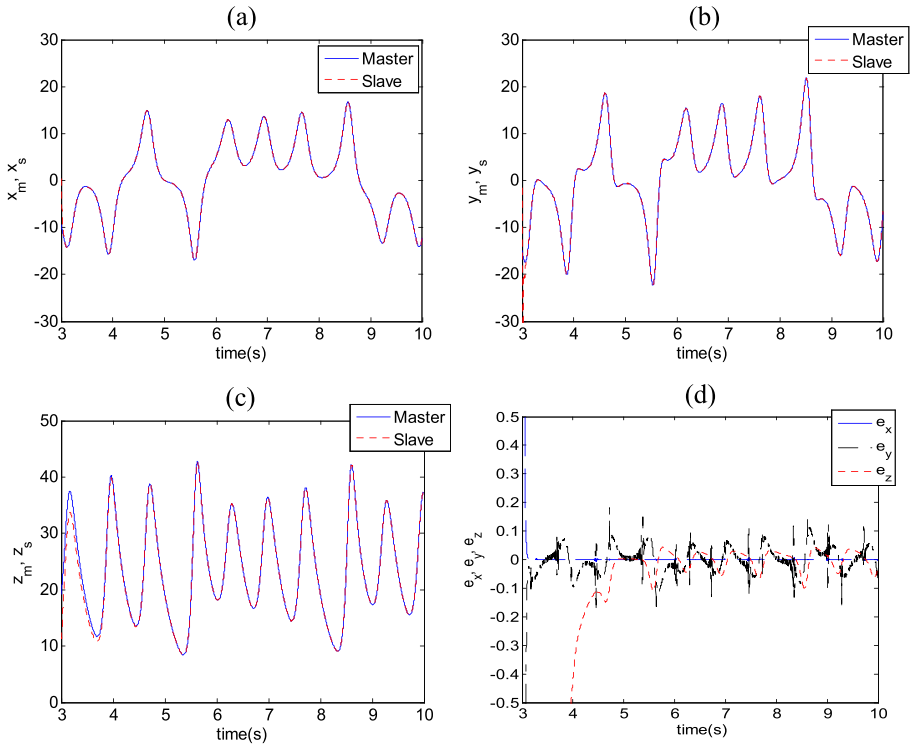

Figure 4. Time evolutions of the master and slave systems: (a) x_m and x_s, (b) y_m and y_s, (c) z_m and z_s. (d) Synchronization errors. [Colour figure can be viewed at wileyonlinelibrary.com]

$$\begin{aligned}\dot{x}' &= G_T\left\{\sigma\left(y' - x'\right)\right\},\\ \dot{y}' &= G_T\left\{rx' - y' - 10x'z'\right\},\\ \dot{z}' &= G_T\left\{10x'y' - bz'\right\}.\end{aligned} \tag{46}$$

Four operational amplifiers (LF412, National Semiconductor) and associated circuitry perform operations of sum, multiplication and integration. Two analog multipliers (AD633, Analog Devices) implement the quadratic terms in the circuit equations. A set of state equations that govern the dynamical behavior of the circuit is obtained as

$$\begin{aligned}\dot{x}' &= \frac{R_5}{C_{p1}}\left(\frac{1}{R_1}y' - \frac{1}{R_2}x'\right),\\ \dot{y}' &= \frac{1}{C_{p2}}\left(\frac{1}{R_3}x' - \frac{1}{R_5}y' - \frac{1}{10{\cdot}R_4}x'z'\right),\\ \dot{z}' &= \frac{1}{C_{p3}}\left(\frac{1}{10{\cdot}R_4}x'y' - \frac{1}{R_7}z'\right).\end{aligned} \tag{47}$$

For setting $\sigma = 10$, $r = 28$, $b = 8/3$, the resistors are selected as

$$R_1 = R_2 = 100, R_3 = 36, R_4 = 10, R_5 = 1000, R_6 = 10, R_7 = 374 \ \ (k\Omega).$$

The capacitors are selected as

$$C_{p1} = C_{p2} = C_{p3} = 47 \ \ (n\mathrm{F}).$$

The Lorenz circuit has a bandwidth of signal x' in about 0 – 120 Hz. The time-scaling factor G_T of this circuit is estimated as 22. A digital signal processor (DSP, TMS320F2812, Texas

DOI: 10.1002/cta

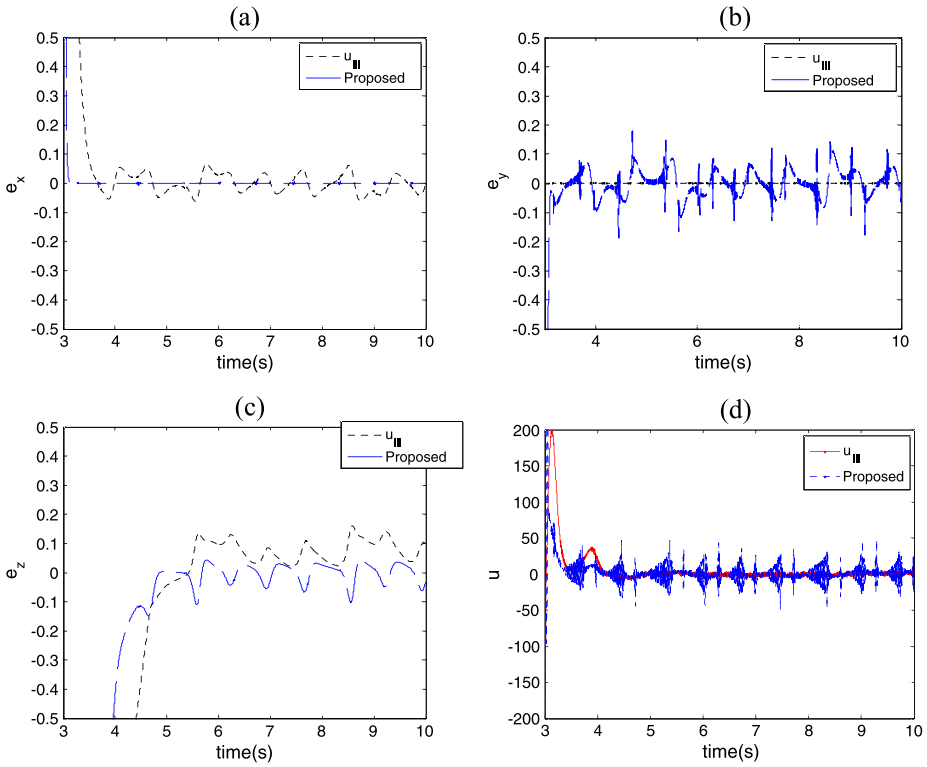

Figure 5. Time evolutions of (a) error state e_x, (b) error state e_y, (c) error state e_z and (d) control inputs under the control in [25] and proposed control. The controllers are activated at 3 s. [Colour figure can be viewed at wileyonlinelibrary.com]

Instruments) and TMS320F28X EVM (Texas Instruments) are used for signal processing. Signal conditioning circuits are also considered for ADC (analog-to-digital converter) inputs to remain in the range of 0 – 3 V and DAC (digital-to-analog converter) inputs to remain in the range of 0 – 4.096 V. A schematic and picture of the experimental settings are shown in Figures 6 and 7.

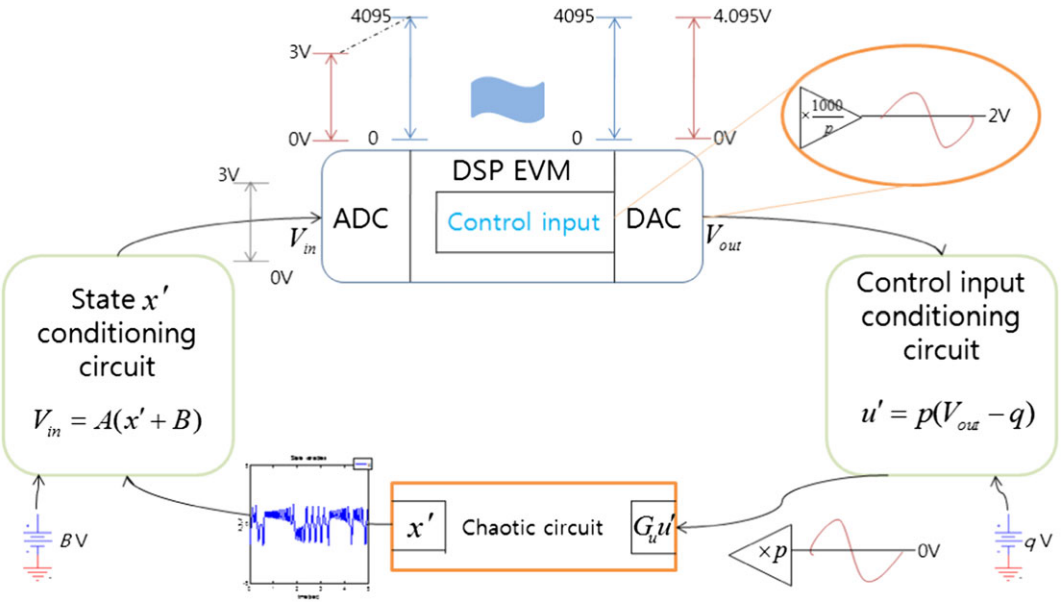

Figure 6. Schematic diagram of control with a DSP EVM. [Colour figure can be viewed at wileyonlinelibrary.com]

DOI: 10.1002/cta

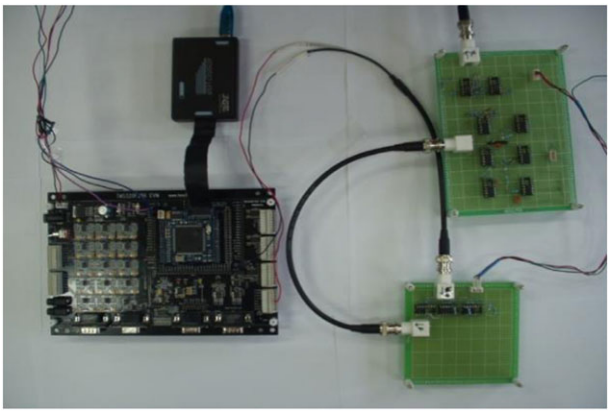

Figure 7. Overall implementation for control of a chaotic circuit. [Colour figure can be viewed at wileyonlinelibrary.com]

The control objective is to regulate x' to 1 V. In the control law (16), control gain $\overline{B}$ is tuned to 90 000, and C_1 and C_2 are both set as 350. The sampling frequency is set as 2 kHz to be sufficiently larger than the Nyquist frequency 240 Hz.

Figure 8a and b show the waveforms of state x' and its corresponding control input u' from the Lorenz circuit, which are measured by an oscilloscope, respectively. The control input is activated at $t = 0.4$. It is observed that state x' intends to converge to 1 V. However, the vibration of signal x' is displayed in steady state. The factors that lead to the vibrations at steady state include unstable power supply to the DSP, ADC resolutions and external noise.

4.2. Synchronization of the Lorenz systems

Next, we conduct synchronization between two identical Lorenz circuits. First, for the control input (40), gain $\overline{B}$ is tuned to 250 000. C_1 and C_2 are both set as 550. And the sampling frequency is set as 3.33 kHz. The experiment results show that state x' of the slave system follows state x'_d of the master system, as shown in Figure 9a and b. Figure 10 displays the control input measured by an oscilloscope.

Uncertainties in the experiments result from external noise, unstable power supply to the DSP and tolerances of the electronic elements including resistors and capacitors. In particular, in the case of synchronization, the two chaotic circuits are not exactly identical due to the tolerances, which give parameter variations. The synchronization error is measured as 33 – 66 mV, while the magnitude of the desired trajectory rises up to 2.32 V. Even in the presence of those uncertainties, we observe that the proposed control achieves synchronization between the two Lorenz circuits.

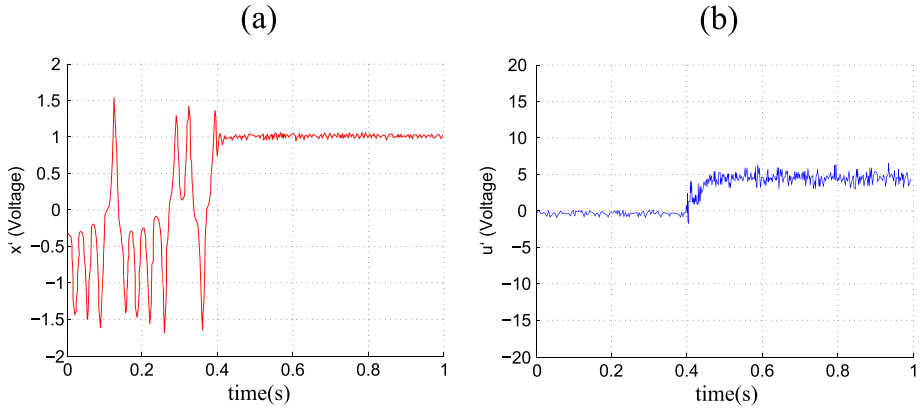

Figure 8. Experiment results: time evolutions of (a) state x' and (b) control input u'. [Colour figure can be viewed at wileyonlinelibrary.com]

DOI: 10.1002/cta

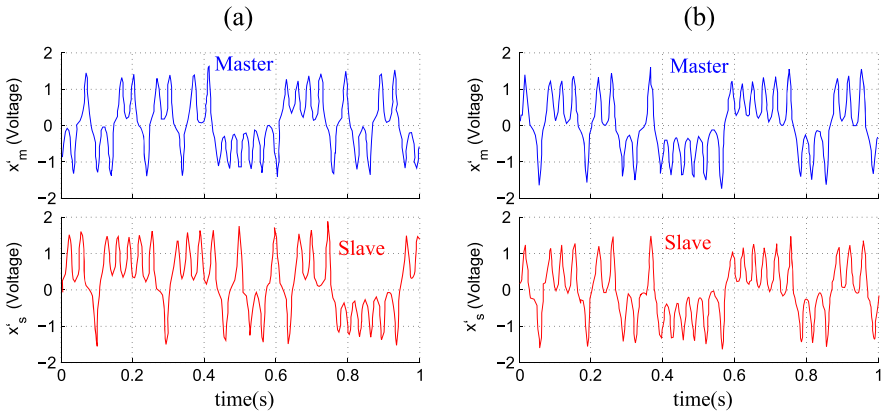

Figure 9. Time evolutions of states $x_m^{'}$ and $x_s^{'}$ (a) before and (b) after synchronization. [Colour figure can be viewed at wileyonlinelibrary.com]

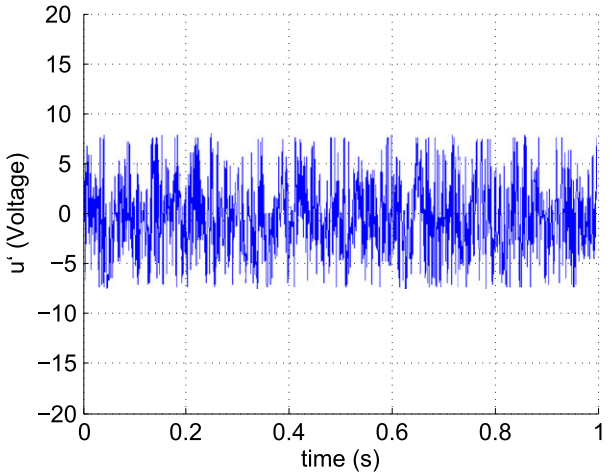

Figure 10. Time evolutions of control input $u^{'}$ for synchronization. [Colour figure can be viewed at wileyonlinelibrary.com]

5. CONCLUSION

We have proposed a robust backstepping technique using TDE to regulate and synchronize the GLS that contains the Lorenz system, Chen system and Lü system. The control technique provides a single controller that can be applied to any chaotic systems in strict feedback form for regulation and synchronization, even if a precise model is unavailable. Mismatched uncertainties are managed by multiple TDEs. Numerical simulation results demonstrate fast, accurate and robust performance of the proposed technique in the presence of matched, mismatched disturbances and parameter variations. The proposed technique is experimentally verified with physical chaotic systems constructed by analog circuit elements. The experimental results show satisfactory performances.

ACKNOWLEDGEMENT

The research for Professor Chang was supported by the DGIST R&D Program of the Ministry of Education, Science and Technology of Korea(11-IT-01).

REFERENCES

1. Kim D et al. Control and synchronization of Lorenz systems via robust backstepping technique. *12th International Conference on Control, Automation and Systems (ICCAS)* 2012; 328–332.

DOI: 10.1002/cta

2. Andrievskii BR, Fradkov AL. Control of chaos: methods and applications. II. Applications. *Automation and Remote Control* 2004; **65**(4):505–533.
3. Wang Q et al. Theoretical design and FPGA-based implementation of higher-dimensional digital chaotic systems. *IEEE Transactions on Circuits and Systems I* 2016; **63**(3):401–412.
4. Chen C, Chen H. Robust adaptive neural-fuzzy-network control for the synchronization of uncertain chaotic systems. *Nonlinear Analysis: Real World Applications* 2009; **10**(3):1466–1479.
5. Rulkov NF, Tsimring LS. Synchronization methods for communication with chaos over band-limited channels. *International Journal of Circuit Theory and Applications* 1999; **27**(6):555–567.
6. Chen F, Chen L, Zhang W. Stabilization of parameters perturbation chaotic system via adaptive backstepping technique. *Applied Mathematics and Computation* 2008; **200**(1):101–109.
7. Cui F et al. Bifurcation and chaos in the Duffing oscillator with a PID controller. *Nonlinear Dynamics* 1997; **12**(3):251–262.
8. Gambino G, Lombardo MC, Sammartino M. Global linear feedback control for the generalized Lorenz system. *Chaos, Solitons & Fractals* 2006; **29**(4):829–837.
9. Ge SS, Wang C, Lee TH. Adaptive backstepping control of a class of chaotic systems. *International Journal of Bifurcation and Chaos* 2000; **10**(5):1149–1156.
10. Layeghi H et al. Stabilizing periodic orbits of chaotic systems using fuzzy adaptive sliding mode control. *Chaos, Solitons & Fractals* 2008; **37**(4):1125–1135.
11. Liao T, Lin S. Adaptive control and synchronization of Lorenz systems. *Journal of the Franklin Institute* 1999; **336**(6):925–937.
12. Naseh MR, Haeri M. An optimal approach to synchronize non-identical chaotic circuits: an experimental study. *International Journal of Circuit Theory and Applications* 2011; **39**(9):947–962.
13. Noroozi N, Roopaei M, Jahromi MZ. Adaptive fuzzy sliding mode control scheme for uncertain systems. *Communications in Nonlinear Science and Numerical Simulation* 2009; **14**(11):3978–3992.
14. Park C, Lee C, Park M. Design of an adaptive fuzzy model based controller for chaotic dynamics in Lorenz systems with uncertainty. *Information Sciences* 2002; **147**(1):245–266.
15. Zeng Y, Singh SN. Adaptive control of chaos in Lorenz system. *Dynamics and Control* 1997; **7**(2):143–154.
16. Wu Z et al. Sampled-data fuzzy control of chaotic systems based on a T–S fuzzy model. *IEEE Transactions on Fuzzy Systems* 2014; **22**(1):153–163.
17. Zhang L et al. Fuzzy adaptive synchronization of uncertain chaotic systems via delayed feedback control. *Physics Letters A* 2008; **372**(39):6082–6086.
18. Čelikovský S, Chen G. On the generalized Lorenz canonical form. *Chaos, Solitons & Fractals* 2005; **26**(5):1271–1276.
19. Wang Y et al. Adaptive synchronization of GLHS with unknown parameters. *International Journal of Circuit Theory and Applications* 2009; **37**(8):920–927.
20. Wu X, Cai J, Zhao Y. Some new algebraic criteria for chaos synchronization of Chua's circuits by linear state error feedback control. *International Journal of Circuit Theory and Applications* 2006; **34**(3):265–280.
21. Yu Y, Zhang S. Adaptive backstepping synchronization of uncertain chaotic system. *Chaos, Solitons & Fractals* 2014; **21**(3):643–649.
22. Wang T et al. Adaptive fuzzy backstepping control for a class of nonlinear systems with sampled and delayed measurements. *IEEE Transactions on Fuzzy Systems* 2015; **23**(2):302–312.
23. Niu Y, Wang X. A novel adaptive fuzzy sliding-mode controller for uncertain chaotic systems. *Nonlinear Dynamics* 2013; **73**(3):1201–1209.
24. Jin M, Chang P. Simple robust technique using time delay estimation for the control and synchronization of Lorenz systems. *Chaos, Solitons & Fractals* 2009; **41**(5):2672–2680.
25. Kim D, Gillespie RB, Chang PH. Simple, robust control and synchronization of the Lorenz system. *Nonlinear Dynamics* 2013; **73**(1–2):971–980.
26. Čelikovský S, Vaněček A. Bilinear systems and chaos. *Kybernetika* 1994; **30**(4):403–424.
27. Čelikovský S, Chen G. On a generalized Lorenz canonical form of chaotic systems. *International Journal of Bifurcation and Chaos* 2002; **12**(8):1789–1812.
28. Lorenz EN. Deterministic nonperiodic flow. *Journal of the Atmospheric Sciences* 1963; **20**(2):130–141.
29. Chen G, Ueta T. Yet another chaotic attractor. *International Journal of Bifurcation and Chaos* 1999; **9**(7):1465–1466.
30. Lü J, Chen G. A new chaotic attractor coined. *International Journal of Bifurcation and Chaos* 2002; **12**(3):659–661.
31. Chen D et al. Circuit implementation and model of a new multi-scroll chaotic system. *International Journal of Circuit Theory and Applications* 2014; **42**(4):407–424.
32. Li Y, Tang WKS, Chen G. Hyperchaos evolved from the generalized Lorenz equation. *International Journal of Circuit Theory and Applications* 2005; **33**(4):235–251.
33. Li Y et al. A new hyperchaotic Lorenz-type system: generation, analysis, and implementation. *International Journal of Circuit Theory and Applications* 2011; **39**(8):865–879.
34. Jafari S, Haeri M, Tavazoei MS. Experimental study of a chaos-based communication system in the presence of unknown transmission delay. *International Journal of Circuit Theory and Applications* 2010; **38**(10):1013–1025.
35. Youcef-Toumi K, Ito O. A time delay controller for systems with unknown dynamics. *Journal of Dynamic Systems, Measurement, and Control* 1990; **112**(1):133–142.
36. Hsia TC, Lasky TA, Guo Z. Robust independent joint controller design for industrial robot manipulators. *IEEE Transactions on Industrial Electronics* 1991; **38**(1):21–25.

DOI: 10.1002/cta

37. Jin M, Lee J, Chang PH, Choi C. Practical nonsingular terminal sliding-mode control of robot manipulators for high-accuracy tracking control. *IEEE Transactions on Industrial Electronics* 2009; **56**(9):3593–3601.
38. Jin M, Kang SH, Chang PH. Robust compliant motion control of robot with nonlinear friction using time-delay estimation. *IEEE Transactions on Industrial Electronics* 2008; **55**(1):258–269.
39. Jin M, Lee J, Tsagarakis N. Model-free robust adaptive control of humanoid robots with flexible joints. *IEEE Transactions on Industrial Electronics* 2017; **64**(2):1706–1715.
40. Jin M, Lee J, Ahn KK. Continuous nonsingular terminal sliding-mode control of shape memory alloy actuators using time delay estimation. *IEEE/ASME Transactions on Mechatronics* 2015; **20**(2):899–909.
41. Jin Y et al. Stability guaranteed time delay control of manipulators using nonlinear damping and terminal sliding mode. *IEEE Transactions on Industrial Electronics* 2013; **60**(8):3304–3317.
42. Hsia TC, Gao LS Robot manipulator control using decentralized linear time-invariant time-delayed joint controllers. *Proceedings IEEE International Conference on Robotics and Automation*, 1990. 2070–2075.
43. Kim D et al. Control and synchronization of Lorenz systems via robust backstepping technique. *12th International Conference on Control, Automation and Systems (ICCAS)*, 2012. 328–332.

DOI: 10.1002/cta